Ice load penetration modelling

Riska, K.; Frederking, R. M. W.

Proceedings: POAC-87: 9th Port and Ocean Engineering under Arctic Conditions Conference: 17 August 1987, Fairbanks, Alaska, USA, 1, pp. 317-327, 1987-08-17

National Research Council Canada
Conseil national de recherches Canada

Institute for Research in Construction
Institut de recherche en construction

Ice Load Penetration Modelling

by K. Riska and R. Frederking

Appeared in
Proceedings of the Ninth Port and Ocean
Engineering Under Arctic Conditions Conference (POAC-87)
Fairbanks, Alaska, August 17-21, 1987
Vol. I, p. 317-327
(IRC Paper No. 1560)

Reprinted with permission of the
Geophysical Institute, University of Alaska
Fairbanks, Alaska

NRCC 29413

Canada

RÉSUMÉ

Un programme d'essais en laboratoire a été mené pour mesurer la déformation et la résistance de la glace de plusieurs années à des températures de -2, -10 et -20 °C. Le lien entre la vitesse de déformation et la résistance dans l'intervalle de 10^{-6} s^{-1} à 10^{-2} s^{-1} a été établi pour des conditions de charge uniaxiale, biaxiale et triaxiale. Ces données ont été ajustées au moyen d'une analyse de régression à une surface de rupture. Le critère de Tsai-Wu s'est révélé le plus satisfaisant pour décrire cette surface.

Un modèle de pénétration basé sur des coefficients de contact proposés par Varsta a été formulé pour décrire physiquement le processus de pénétration. Les coefficients ont été déterminés empiriquement à partir de données d'essai à deux échelles. Le modèle de pénétration fait le lien entre la pression moyenne réelle (p_{av}) s'exerçant sur la surface de contact (A) et une pression de la glace nominale (p_{nom}) calculée à partir des propriétés de la glace et de la géométrie de pénétration. La distribution des contraintes au sein de la glace pour la géométrie de pénétration est déterminée par une méthode d'éléments finis.

Un numéro de contrainte de référence qui relie l'état de contrainte à l'état de contrainte de rupture permet de déterminer la contrainte nominale exercée sur la surface de contact au début de la rupture de la glace. Une relation empirique de la forme $p_{av} - C\,(A/A_o)^n\,p_{nom}$ représente bien la pression moyenne sur la surface de contact pendant la pénétration de la structure dans la glace. La valeur de l'exposant n était de -0,41 pour les pénétration à grande et à petite échelles.

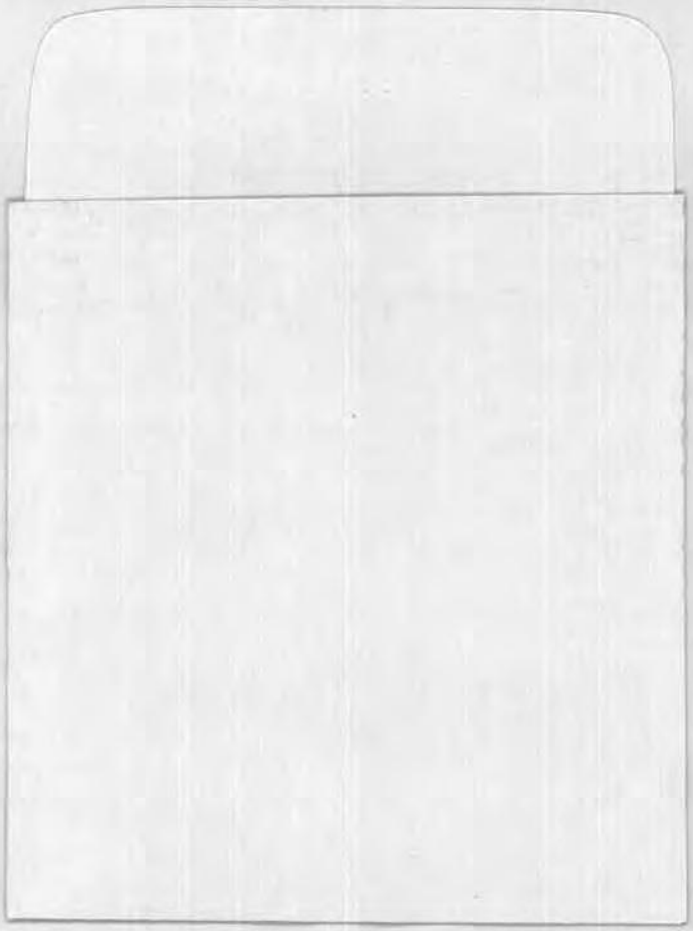

ICE LOAD PENETRATION MODELLING

K. Riska
Technical Research Centre of Finland, Espoo, FINLAND

R. Frederking
National Research Council, Ottawa, Ontario, CANADA

Abstract

A laboratory test program was conducted to measure the deformation and strength properties of multi-year ice at temperatures of -2, -10 and -20°C. The strain rate dependence of strength over the range 10^{-6} s^{-1} to 10^{-2} s^{-1} was determined for uniaxial, biaxial and triaxial loading conditions. These data were fit by means of a regression analysis to a failure surface. The Tsai-Wu criterion was found to be most satisfactory for describing this surface.

A penetration model based on contact coefficients as suggested by Varsta was formulated to physically describe the penetration process. The coefficients were determined empirically from test data at 2 scales. The penetration model relates the actual average pressure (p_{av}) acting on the contact area (A) to a nominal ice pressure (p_{nom}) calculated from ice properties and the penetration geometry. The stress distribution within the ice for the penetration geometry is determined with a finite element method.

This is a reviewed and edited version of a paper presented at the Ninth International Conference on Port and Ocean Engineering Under Arctic Conditions, Fairbanks, Alaska, USA, August 17-22, 1987.

A reference stress number which relates the stress state to the failure stress state is used to determine the nominal stress on the contact surface for the onset of failure of the ice. An empirical relation of the form $p_{av} = C\,(A/A_o)^n\,p_{nom}$ was found to represent the average pressure on the contact surface during structure penetration into ice. The value of the exponent n was -0.41 for both large and small scale penetration.

Introduction

Ice forces generated on a structure arise from the relative movement of the ice feature with respect to the structure. If the movements are small or slow they may be accommodated by elastic or creep deformation within the ice feature. In many cases, however, the structure penetrates into the ice feature with an accompanying total disintegration of the ice. This is the loading process which will be addressed in this paper.

There are two ice load penetration cases of interest. The first one, that of a ship penetrating into an infinite ice feature, results in a contact geometry such that the contact area increases throughout the penetration process, with the highest load occurring at the end of the penetration.

Generally, the penetrating structure (ship's bow) is inclined to the direction of movement. This scenario has led to an ice force formulation where the ice pressure is assumed to decrease with increasing contact area; the so called pressure-area relation (Sanderson, 1984). The other case is of an ice sheet indenting a fixed vertical-faced structure (pile) where the contact geometry remains constant throughout the process. The maximum load occurs when the structure is completely enveloped by the ice. In this scenario, the ice force formulation is assumed to show the maximum load to decrease with increasing ratio of ice thickness to structure width; the so called indentation coefficient-aspect ratio effect (Afanasev et al, 1971). This latter formulation was developed by Korzhavin (1971) and related the maximum ice pressure to a form factor, a contact factor, an indentation coefficient and the uniaxial compressive strength of the ice. Maximum ice force was obtained by multiplying the ice pressure by the contact area.

The case of a structure penetrating into an ice feature has been studied more as an interaction process since the maximum pressure, indentation and load are a function of the size and velocity of the vessel as well as the properties of the ice. Varsta (1983) carried out laboratory measurements of ice pressure generated during increasing contact area penetration with a crushing mode of failure. This led to a formulation of average ice pressure based on a contact coefficient which varies during the penetration process.

Both of the above cases are based on essentially empirical factors and are thus difficult to generalize. There is a real need for an ice force formulation based on an understanding of the physical processes involved. This formulation would take into account the geometry of the structure and the appropriate deformation and strength properties of the ice.

The objective of this paper is to indicate how to incorporate ice strength into analytical models for ice pressure during penetration. Multi-year ice strength data will be presented and then incorporated into a failure criterion from which a nominal contact pressure can be calculated for a particular penetration geometry. This nominal ice pressure, together with an empirical contact coefficient, can be used to predict average contact pressure during the penetration process.

Development of Failure Criterion for Isotropic Ice

The overall approach here was to determine strength properties of isotropic ice for different stress combinations and loading orientations. The testing was concentrated in the compression-compression-compression octant as the intended applications were in this zone. Because more data are available than the minimum required for describing the failure criterion, a regression approach was used to obtain the best fit.

Strength tests

The ice used for these tests was recovered from the eastern Canadian Arctic. Block samples were recovered from two multi-year floes frozen into the landfast ice adjacent to the south shore of Lancaster Sound. One was tabular in form, about 30 by 50 m in size and grounded in 10 m of water. The other was an irregular block about 5 m across and grounded at the shore line. The temperature of the ice at the time of sampling was about -30°C. After transporting to the south it was stored in a cold room at -10° to -20°C.

Three different series of tests were carried out. These included uniaxial and biaxial (confined) compression tests at the National Research Council of Canada (NRCC) in Ottawa and triaxial compression tests performed (under contract) by Geotech in Calgary. Grain structure of the ice was examined by placing thin sections of the ice between crossed polarized sheets. The tabular floe had a variable grain structure which could be described as type R, agglomerate (Michel and Ramseier, 1971). The other floe had a more columnar structure, but was still variable. It fit the description of "breccia" by Richter and Cox (1984). The

average density of the tabular ice floe was 875 kg/m^3 and the block 900 kg/m^3. Salinity of the ice tested at NRCC ranged from 1.2 to 3.0 °/₀₀ while that tested at Geotech was 0.1 to 0.3 °/₀₀. This lower value may have been due to brine drainage during transportation.

Prismoidal specimens 250 mm long by 100 mm wide and 100 mm thick for the uniaxial and 70 mm thick for the biaxial tests were used. For the triaxial tests cylinders 250 mm long by 95 mm in diameter were used. All testing was carried out on servo hydraulic machines with closed loop control on strain rate. For the uniaxial and biaxial tests an extensometer was attached directly to the specimen to provide the control signal. In the case of the triaxial tests, relative movement between the load platens was used for control, in addition to the confining pressure which was maintained at a constant ratio to the axially applied stress. More details on the test procedures can be found in Riska and Frederking (1987).

Testing was carried out at temperatures of -2°, -10° and -20°C, and at strain rates ranging from 10^{-6} s^{-1} to 10^{-2} s^{-1}. For strain rates less than 10^{-4} s^{-1} the mode of failure was ductile with an upper yield strength. For higher rates the stress-strain curve was linear up to an abrupt failure. This behaviour is illustrated in Figure 1 for tests at a temperature of -10°C. It can be seen that at a strain rate of 10^{-2} s^{-1} the curve is linear up to failure, but that the slope of the curve, 8.5 GPa is still less than the Young's Modulus value of about 9.5 GPa. The results of the uniaxial and biaxial tests are summarized in Figures 2 and 3. These results show an increase in strength with increasing strain rate for the ductile mode of failure similar to that found for fresh water ice by Gold and Krausz (1971). For strain rates of about 10^{-3} s^{-1} and higher the failure behaviour is brittle and there is no consistent dependence of strength on strain rate. This region has been termed one of premature failure (Sinha, 1981). The actual failure strength is most likely influenced by small imperfections in the ends of the specimens. While there is doubt about the actual strength values the ice behaviour preceding premature failure can be described as linearly elastic. Figure 4 summarizes the results of the triaxial testing which was carried out under proportionate loading.

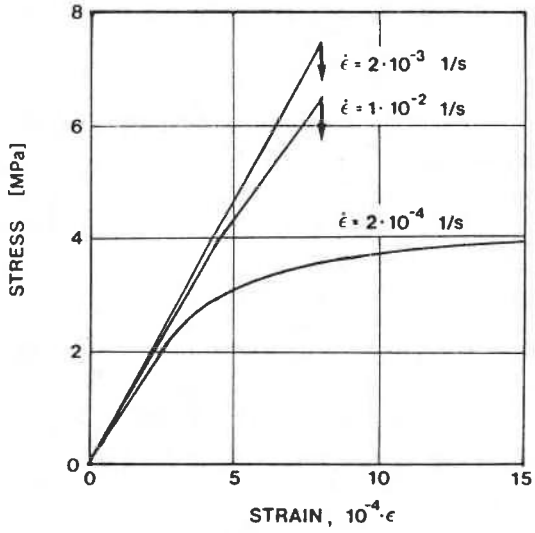

Figure 1. Stress vs strain for constant strain rate uniaxial compressive strength of multi-year ice at -10°C.

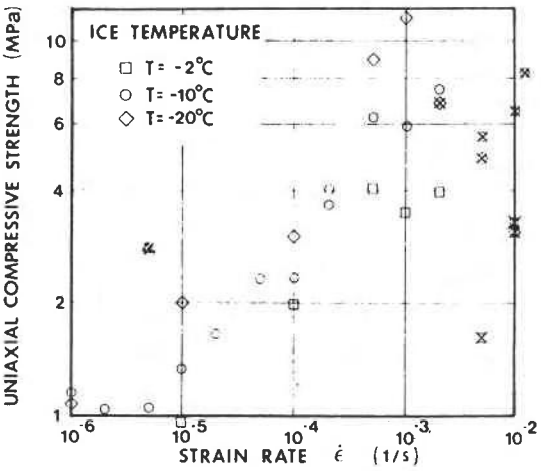

Figure 2. Uniaxial compressive strength of multi-year ice. Tests in which the ice failed prematurely are crossed.

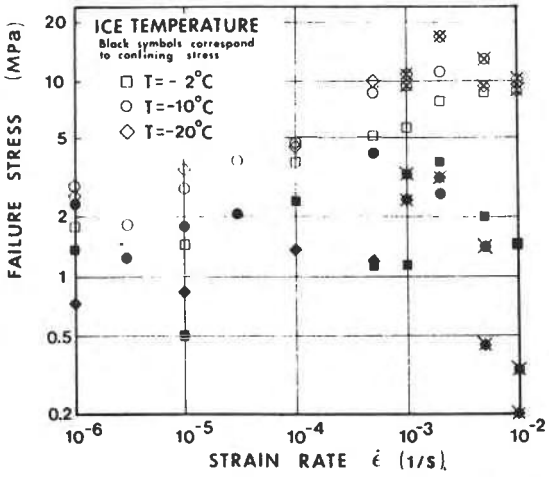

Figure 3. Strength results from confined compression (biaxial) tests. The crossed results correspond to premature failure.

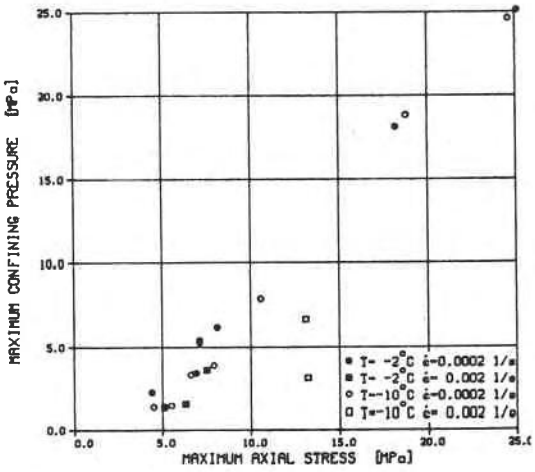

Figure 4. Results from triaxial compression tests.

Formulation of a failure surface

The onset of failure in a continuous material is usually described by either a yield or failure criterion. Both criteria define a stress region within which the material does not fail. This region is represented by the formula

$$f(\sigma) < 1 \qquad (1)$$

where f is the yield or failure function of the six independent stress components σ. The surface $f(\sigma) = 1$ is called the failure surface or envelope. The difference between a failure and a yield criterion is that yield is generally associated with plastic behaviour and failure with brittle behaviour. The same material may exhibit either behaviour depending on temperature and strain rate. The difference between the failure and yield surface is illustrated schematically in Figure 5.

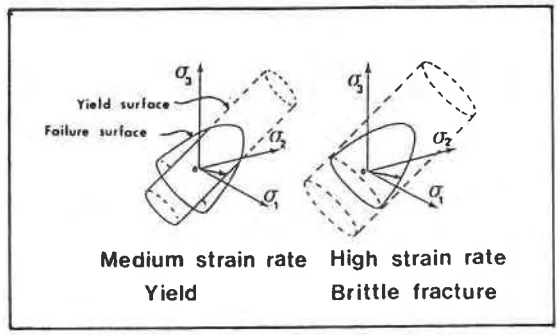

Figure 5. Schematic presentation of the difference between yield and failure surfaces. The vector from the origin shows the stress path to yield or failure.

The failure function $f(\sigma)$ is a scalar and consequently it can be expressed as a function of solely the three invariants of the stress tensor I_i, $i = 1, 2, 3$, or

$$f(I_1, I_2, I_3) < 1 \qquad (2)$$

where the invariants can be in terms of the stress components σ_{ij} or principal stresses σ_i $(i = j = 1, 2, 3)$. Equation

(2) is valid only if the material is isotropic; i.e. the stress components are independent of the orientation of the coordinate system. As discussed earlier, multi-year ice is considered to be isotropic at the scale of the structure/ice penetration problem.

There are two requirements for an isotropic failure criterion of multi-year ice; i) the ability to account for different tensile and compressive strengths and, ii) adequately describe the increased strength in multiaxial compressive stress states. A very general criterion is that of Tsai and Wu (1971) which has a quadratic form

$$f(\sigma) = \sum_{i,j} F_{ij}\,\sigma_{ij} + \sum_{i,j,k,l} G_{ijkl}\,\sigma_{ij}\,\sigma_{kl} \qquad (3)$$

where F_{ij} and G_{ijkl} are second and fourth order strength tensors. In an isotropic case presented with principal stresses Riska and Frederking (1987) showed this criterion reduces to

$$f(\sigma) = F_{11}\,I_1 + \frac{1}{3}\,(G_{1111} + 2\,G_{1122})\,I_1^2 + 4\,G_{1212}\,J_2 \qquad (4)$$

where J_2 is the second invariant of the deviatoric stress. This is essentially a three parameter criterion since $G_{1212} = \frac{1}{2}(G_{1111} - G_{1122})$. Recently another three parameter criterion based partly on physical reasoning has been proposed by Nadreau and Michel (1986). It has the form

$$f(\sigma) = aI_1^3 + bI_1^2 + cI_1 + dJ_2 \qquad (5)$$

where a, b, c, and d are derived from a knowledge of T and C, tensile and compressive strengths under the hydrostatic stress state and θ is a fitting parameter related to the stress level required to induce pressure melting at a given temperature.

Either of the failure criteria obtained are macroscopic ones. They predict only the maximum stress state the material can sustain and consequently the maximum load ice can exert on a structure. They do not predict the behaviour of the material once the stress reaches the failure state. This is an area where fracture mechanics may be a fruitful approach.

Failure surface determination for the test cases

The determination of strength constants requires selection of these values so that the failure surface best fits a set of measured strength values. A number of sets were obtained for different ice temperatures and strain rates. For illustrative purposes, data group IV for -10°C and 2×10^{-3} s^{-1} is presented in Table 1. Note that all the data in Table 1 are for compressive stresses.

Where more data than the minimum data required to determine the coefficients in equations (4) or (5) are available a regression is performed to obtain the best fit. This is done by minimizing the following function over the independent parameters

$$L = \sum_i (\lambda_i - 1)^2 \qquad (6)$$

where λ is the strength number corresponding to the i'th strength measurement. The strength number for the Tsai-Wu criterion is

$$\lambda = \frac{2\,B_i}{\sqrt{A_i^2 + 4\,B_i} - A_i} \qquad (7)$$

where $B_i = \left(\frac{I_{1_i}^2}{3} + J_{2_i}\right) G_{1111} + \left(\frac{2}{3}\,I_{1_i}^2 + 2\,J_{2_i}\right) G_{1122}$

$$A_i = F_{11}\,I_{1_i}$$

and I_{1_i} and J_{2_i} are the stress invariants for the i'th measurement. It is also

Table 1. Strength test results used in determination of failure surface

σ_1 [MPa]	σ_2 [MPa]	σ_3 [MPa]
Data set I; -2°C, 0.0002 s^{-1}		
2.4	0	0
3.2	0	0
5.2	1.1	0
3.9	2.4	0
8.0	5.9	5.9
4.9	2.4	2.4
20.4	20.4	20.4
6.7	5.0	5.0
5.7	2.8	2.8
20.7	20.7	20.7
Data set II; -2°C, 0.002 s^{-1}		
4.0	0	0
4.2	0	0
8.8	2.0	0
7.9	3.9	0
5.8	1.2	0
6.0	2.8	2.8
4.2	1.1	1.1
5.2	1.3	1.3
Data set III; -10°C, 0.0002 s^{-1}		
5.0	0	0
3.7	0	0
4.0	0	0
2.8	0	0
8.7	4.3	0
4.8	2.4	0
11.8	8.8	8.8
7.7	3.8	3.8
20.4	20.4	20.4
8.7	6.5	6.5
6.5	3.2	3.2
4.6	1.1	1.1
3.7	1.1	1.1
20.3	20.3	20.3
Data set IV; -10°C, 0.002 s^{-1}		
7.5	0	0
7.0	0	0
5.8	0	0
8.2	0	0
13.0	1.5	0
11.3	2.7	0
9.6	3.4	0
10.8	5.4	5.4
10.9	2.5	2.5

possible to derive the strength number for the Nadreau criterion. The regression gave a flat minimum when applied to either criterion. Because the different failure surfaces differed only in the tensile quadrant it was decided that the calculation could be performed more easily by fixing the tensile strength S_T. This allowed the elimination of one independent parameter from the regression. For the Tsai-Wu criterion

$$F_{11} = \frac{1 - G_{1111} S_T^2}{S_T} \qquad (8)$$

and for the Nadreau criterion

$$\tan\theta = \frac{(C + T)\ 2\ S_T^2}{9\ TC^2\ (1 - aS_T^3 - bS_T^2 - cS_T} \qquad (9)$$

The value of S_T, if in the range 0.5 to 1.5 MPa, did not have much influence on the root mean square error at the minimum of equation (7). A value of S_T = 0.9 MPa was chosen.

The regression of equation (7), taking into account equations (8) and (9), gives the results presented in Table 2. The final failure surfaces can be visualized by drawing the intersection of the surface with the $\sigma_1 - \sigma_2$ plane (σ_3 = 0), Figure 6. The differences between the Tsai-Wu and Nadreau criteria are small and thus, in subsequent analysis, the Tsai-Wu criterion will be used solely because of its ease of use and simple extension into anisotropic cases.

The strength number λ used in the regression is also helpful in practical applications of the failure criteria. It can be thought of as a non-dimensional number which defines the ratio of the length of a line from the origin to a point in stress space to the length of a line from the origin to the failure surface and passing through the stress point. In this instance the factors A and B are defined in terms of the stress point σ_{ij} rather than the stress invariants as above. When the strength number is 1 the stress state is on the failure surface and the material fails. The actual method is to assume a unit

Table 2. Results of failure surface regression

		Set I	Set II	Set III	Set IV
Tsai-Wu criterion	F_{11} [MPa^{-1}]	0.736	0.885	0.835	0.988
	G_{1111} [MPa^{-2}]	0.417	0.251	0.307	0.137
	G_{1122} [MPa^{-2}]	-0.188	-0.062	-0.129	-0.024
	S_c [MPa]	2.7	4.4	3.6	8.1
	$(\lambda-1)_{RMS}$	0.35	0.20	0.31	0.14
	P_{HYDR} [MPa]	18.0	7.3	17.1	11.6
Nadreau criterion	C [MPa]	31.4	20.6	30.6	29.5
	T [MPa]	0.736	0.616	0.655	0.563
	$tg^2\theta$	0.026	0.089	0.043	0.138
	S_c [MPa]	2.7	4.4	3.8	8.2
	$(\lambda-1)_{RMS}$	0.29	0.21	0.30	0.15

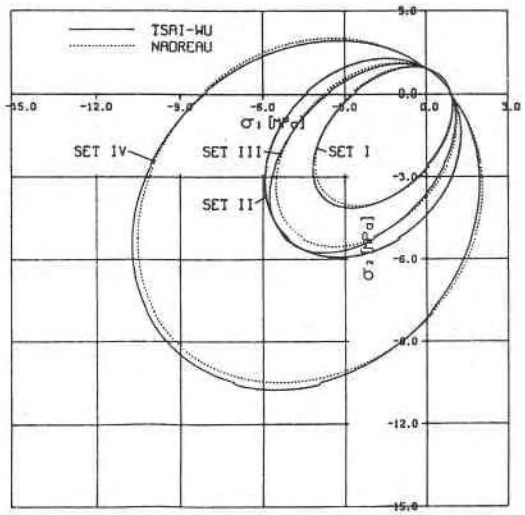

Figure 6. The failure surface on a plane of principal stress. The Tsai-Wu and Nadreau failure surfaces are compared.

boundary load or displacement and then to calculate the values of λ within the body of the material. The unit boundary conditions can then be linearly scaled, either up or down, to give a maximum λ of 1. This method provides an efficient means of incorporating the failure criterion into calculations of the stress state in a body. In actual applications of λ there are some limitations. For example, if the extension of the line through the stress point contacts the failure surface at a point where the surface is far from normal to the line, then small uncertainties in defining the stresses or failure constants could lead to a large variation in the strength number.

Modelling Ice Pressure During Penetration

When a structure penetrates into ice the average ice pressure has been observed to decrease with increasing

penetration (Varsta, 1983). This average ice pressure is defined as the total load divided by the total contact area derived from the geometry of the structure and the depth of the penetration. It is postulated that this average pressure is related to a contact function and a nominal ice pressure

$$p_{av} = g(A,v,,) \; p_{nom} \qquad (10)$$

The contact function, g, has been observed to be a function of contact area. It may be additionally related to indentation speed and aspect ratio, but not ice properties. On the other hand, the nominal pressure is related to the ice properties and the contact geometry. These ideas are here incorporated into an analytical model of ice penetration.

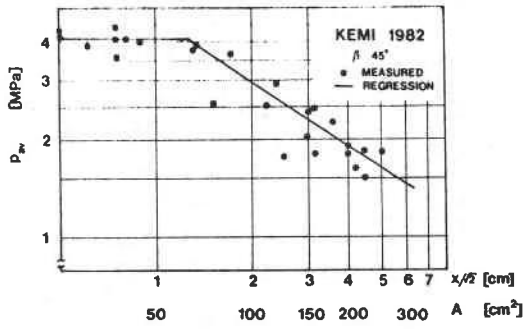

Figure 7. Peak values of ice pressure (p_{av}) as a function of penetration depth z.

Formulation

The nominal ice pressure on the contact surface between a structure and an ice feature is derived from the ice properties and the geometry of the contact. It is the minimum uniform pressure on the ice required to initiate failure; i.e. $\lambda = 1$. This nominal pressure is scale independent and assumes that the ice is intact. There is justification for this assumption from the test results of Varsta (1983) which showed that for the initial stages of penetration of a 45° plane into an ice block, the pressure remained constant with increasing contact area in the early part of the penetration (Figure 7).

The next concept is that of a contact function. This was investigated by Varsta (1983) who proposed that pressure was transmitted through the contact layer by solid-to-solid contact and also a viscous layer. Varsta's results can be interpreted to imply that the contact function varied through the penetration process. It can be described by an empirical relation of the form

$$g(z) = C \; z^n \qquad (11)$$

where z is depth of penetration and C and n are coefficients. Depending on the indentation geometry the contact area varies directly with z or z^2. This formulation ignores velocity which may also effect the contact function.

Calculation of nominal pressure

The actual calculation of the nominal ice pressure can be best demonstrated by an example. Consider the penetration of a ship's bow into an ice feature. The configuration of the contact surface is that of an inclined wedge as shown in Figure 8. The stresses in the ice feature are calculated with the finite element method using three-dimensional solid elements and infinite elements (Klinge, 1985) for the far boundaries. A uniform nominal pressure of 1 MPa is assumed for the calculation and the ice behaviour prior to failure is taken to be linearly elastic. A particular set of ice properties is selected and the yield criterion parameters determined, in this case -10°C and 2×10^{-3} s^{-1} (set IV of Table 2). Within each element of the finite element model the strength number λ is calculated from equation (7) and B and A as defined for the stress state in that element. From these calculations contour plots of λ can be obtained. Figure 9 shows the contours of λ on the contact surface for a uniform nominal ice pressure of 1 MPa. λ values at depth in the ice feature were lower. The maximum value of λ on the contact surface was

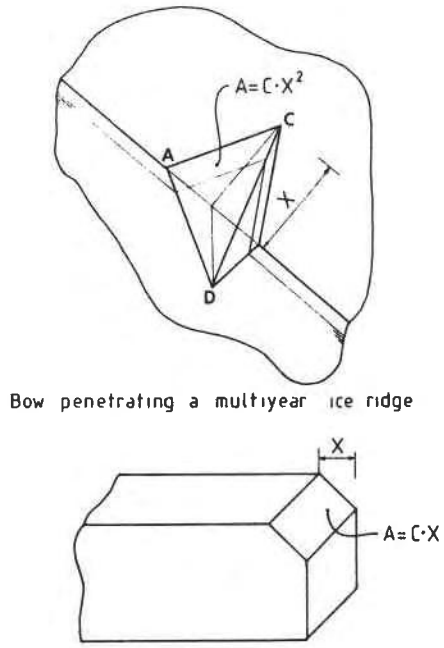

Figure 8. Test configuration of a bow penetrating an idealized multi-year ice feature.

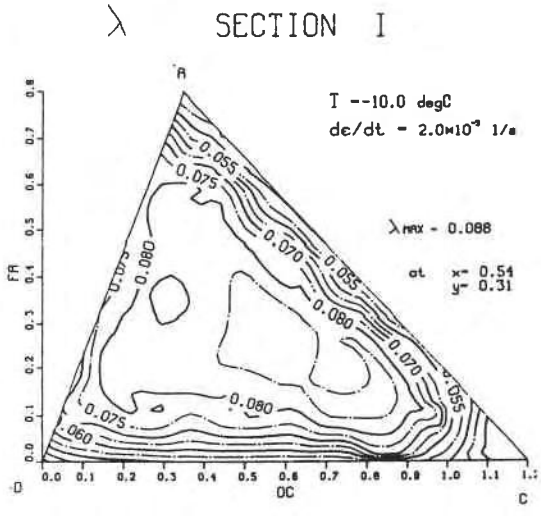

Figure 9. The strength number λ on the contact surface for p_{nom} = 1 MPa. The units for the geometry of the contact are such that the horizontal indentation is unity (distance OC on Fig. 8).

0.088. For the purposes of calculating the nominal pressure, however, the average value of λ is taken to be more representative of the condition of failure on the contact surface. It can also be seen that the λ contours are relatively uniform so that this is not a critical assumption. In this instance the average value of the strength number λ is 0.071, which when scaled up to the failure condition value of 1 gives a uniform nominal ice pressure $p_{nom} = 1/\lambda$ or 14.2 MPa. Results of p_{nom} calculations for the four data sets described in Tables 1 and 2 are summarized in Table 3. It can be seen that higher strain rates and lower temperatures lead to higher values of p_{nom}.

Table 3. P_{nom} values calculated for four sets of data

Set	I	II	III	IV
P_{nom}	8.9	8.4	11.3	14.2 MPa

Contact function

The contact function, g(A, z, v, ..), which could be a function of a number of factors including contact area, A, penetration, z, velocity, v, etc. as discussed previously, will be assumed here to be a function of contact area only

$$g(A) = \frac{p_{av}}{p_{nom}} \qquad (12)$$

where p_{av} and p_{nom} are as defined above. p_{nom} is independent of contact area. p_{av}, on the other hand, has been found to be a function of contact area, A, during the penetration process. Certain data are available from which empirical relations between pressure and contact area can be determined. The resulting contact function calculated from full scale data obtained with the M.V. Arctic

in multi-year ice (Anon, 1985) and laboratory crushing tests (Varsta, 1983) are presented in Figure 10. Regression equations of the contact function give

$$g(A) = 0.1\ (A/A_o)^{-0.42} \qquad (13)$$

for the crushing tests and

$$g(A) = 0.3\ (A/A_o)^{-0.41} \qquad (14)$$

for full scale tests, where $A_o = 1\ m^2$. The value of the exponent is practically the same for two tests of very different geometries. This implies a more general validity of the value of the exponent which characterizes the area dependency. The values of the constant, 0.1 and 0.3, are different which may reflect, for example, the different indentation speeds.

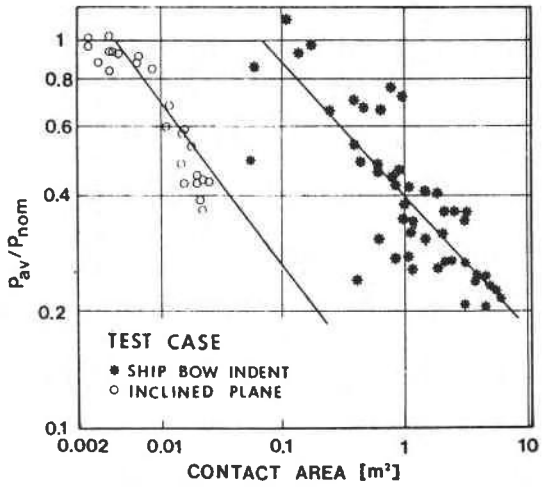

Figure 10. The contact function g(A) plotted vs the contact area for two test cases.

Conclusions

A method has been developed for predicting the average ice pressure on the contact surface during the penetration of a structure into an ice feature. This average pressure is a function of two factors, a nominal ice pressure and a contact function.

The nominal ice pressure can be calculated explicitly by applying an analytical model which requires a knowledge of the geometry of the penetration and the failure surface of the ice. The failure surface can be determined from strength measurements under uniaxial and multiaxial compressive loading. Extensive tests were carried out on multi-year ice and, for strain rates corresponding to ramming tests by ships, behaviour was initially elastic followed by brittle failure. Ice strength was found to be sensitive to multiaxial stress states; i.e. an increase of strength occurred in multiaxial tests compared to uniaxial tests. The ice features from which the ice was sampled could be described as being globally isotropic, although individual specimens did show anisotropy.

The Tsai-Wu failure criterion, which is of a general quadratic form, proved a reasonable fit of a failure surface to the strength data. Starting with elastic behaviour of the ice, a finite element calculation of the stress states in the contact zone was incorporated with the failure criterion through a strength number λ to predict a nominal ice pressure on the contact surface. This is the pressure at which intact ice would fail. For example the nominal ice pressure at $-10°C$ and $2 \times 10^{-3}\ s^{-1}$ was 14 MPa.

To relate this nominal ice pressure to the average pressure on the contact surface during the penetration process an empirical expression (the contact function) of the form $C\ (A/A_o)^n$ was found to provide a good representation. For both small and full scale tests the value of the exponent was about -0.41. The coefficient was 0.1 for small scale tests and 0.3 for full scale tests. There is still not an adequate understanding of the contact function.

A proper physical understanding of ice behaviour in the contact zone is required before a rigorous analytical model can be developed for the contact function. Some of the approaches which

might be taken include treatment of the contact zone as a discontinuous solid/viscous material, application of damage mechanics to the disintegration of the intact ice, and application of non-simultaneous failure concepts.

Acknowledgement

The partial funding of this work, provided in Canada by the Panel on Energy Research and Development through Transport Canada and in Finland by the Ministry of Trade and Industry, is gratefully acknowledged. The continuing interest and support of the project by the Canadian Coast Guard is appreciated. Also the assistance of numerous colleagues at our respective organizations is gratefully acknowledged.

References

Afanasev, V.P., Dolgopolov, Y.V. and Shyeishtein, Z.I. 1971. Ice pressure on separate supporting structures in the sea (in Russian). Arkticheskii i Antarkticheskii Nauchno-Issledovatel'skii. Trudy, Institut, Vol. 300, pp. 61-80. U.S. Army Cold Regions Research and Engineering Laboratory, Hanover, N.H., Draft Translation 346 (1972).

Anon. 1985. M.V. Arctic dedicated field tests: test results and analysis, final report. Prepared for Transport Canada, Coast Guard Northern, by German and Milne and the Technical Research Centre of Finland, Transport Canada Report No. TP6270E.

Gold, L.W. and Krausz, A.S. 1971. Investigation of the mechanical properties of St. Lawrence River ice. Canadian Geotechnical Journal. 8(2): 163-169.

Klinge, P. 1985. Infinite elements (in Finnish). M.Sc. Thesis, Helsinki University of Technology, Espoo, 110 p.

Korzhavin, K. 1971. Action of ice on engineering structures. Cold Regions Research and Engineering Laboratory (CRREL), Draft Translation, Hanover, New Hampshire, 319 p.

Michel, B. and Ramseier, R.O. 1971. Classification of river and lake ice. Canadian Geotechnical Journal. 8: 36-45.

Nadreau, J.P. and Michel, B. 1986. Yield and failure envelope for ice under multiaxial compressive stresses. Cold Regions Science and Technology. 13(1): 75-82.

Richter, J.A. and Cox, G.F.N. 1984. A preliminary examination of the effect of structure on the compressive strength of ice samples from multi-year pressure ridge. Proceedings of Third International Offshore Mechanics and Arctic Engineering Symp., New Orleans, Vol. 3, pp. 140-144.

Riska, K. and Frederking, R. 1987. Modelling ice load during penetration into ice. JRPA No. 1, Ice Load Penetration Model, Report No. 2. Joint Report of the Technical Research Centre of Finland and the National Research Council of Canada. Transport Canada Report No. TP8237E.

Sanderson, T.J.O. 1984. Theoretical and measured ice forces on wide structures. Proceedings of 7th Symposium of Ice Problem, International Association for Hydraulic Research, Hamburg, F.R. Germany, Vol. IV, pp. 151-207.

Sinha, N.K. 1981. Rate sensitivity of compressive strength of columnar- grained ice. Experimental Mechanics. 21(6): 209-218.

Tsai, S. and Wu, E. 1971. A general theory of strength for anisotropic materials. Journal of Composite Materials. 5(1): 58-80.

Varsta, P. 1983. On the mechanics of ice load on ships in level ice in the Baltic Sea. Technical Research Centre of Finland, Publications 11, Espoo, 91 p.